JEM Journal of Experimental Medicine

ARTICLE

CCL22 controls immunity by promoting regulatory T cell communication with dendritic cells in lymph nodes

Moritz Rapp[1], Maximilian W.M. Wintergerst[1], Wolfgang G. Kunz[1], Viola K. Vetter[1], Max M.L. Knott[1], Dominik Lisowski[1], Sascha Haubner[1], Stefan Moder[1], Raffael Thaler[1], Stephan Eiber[1], Bastian Meyer[1], Natascha Röhrle[1], Ignazio Piseddu[1], Simon Grassmann[4], Patrick Layritz[1], Benjamin Kühnemuth[1], Susanne Stutte[7], Carole Bourquin[5,6], Ulrich H. von Andrian[7,8], Stefan Endres[1,2], and David Anz[1,3]

Chemokines have crucial roles in organ development and orchestration of leukocyte migration. The chemokine CCL22 is expressed constitutively at high levels in the lymph node, but the functional significance of this expression is so far unknown. Studying a newly established CCL22-deficient mouse, we demonstrate that CCL22 expression by dendritic cells (DCs) promotes the formation of cell–cell contacts and interaction with regulatory T cells (T reg) through their CCR4 receptor. Vaccination of CCL22-deficient mice led to excessive T cell responses that were also observed when wild-type mice were vaccinated using CCL22-deficient DCs. Tumor-bearing mice with CCL22 deficiency showed prolonged survival upon vaccination, and further, CCL22-deficient mice had increased susceptibility to inflammatory disease. In conclusion, we identify the CCL22–CCR4 axis as an immune checkpoint that is crucial for the control of T cell immunity.

Introduction

Constitutively expressed chemokines control leukocyte trafficking under steady state conditions. These chemokines are crucial for tissue-specific migration and positioning of immune cells within lymphoid organs (Rot and von Andrian, 2004). Mice bearing genetic deficiencies of certain homeostatic chemokines or their receptors have marked defects in lymphoid tissue formation and organ development or show increased sensitivity to infections (Förster et al., 1999; Gunn et al., 1999; Zhou et al., 2006). CCL22 belongs to the group of chemokines that are both constitutively expressed under homeostatic conditions and inducible upon inflammation. The role of inflammatory CCL22 expression is well described: several types of immune cells, such as macrophages, dendritic cells (DCs), B cells, and T cells, secrete CCL22 upon activation (Mantovani et al., 2000; Vulcano et al., 2001). CCL22 is induced by LPS, IL-4, and IL-13 and in T cells by TCR stimulation (Iellem et al., 2000). The only (so far) known receptor of CCL22 is CCR4, which also interacts with a second ligand, the chemokine CCL17 (Campbell et al., 1999; Mantovani et al., 2000).

Upon immune activation, CCR4 is expressed by T helper 2 (Th2)–activated and memory CD4 T cells. CCR4 expression on activated T cells enables their immigration into the skin, predominantly by interaction with CCL17, which is present on dermal blood vessels in the setting of inflammation (Campbell et al., 1999, 2007). In contrast to CCL17, no CCL22 is found on skin endothelial cells. Thus, upon dermal inflammation, CCL17 rather than CCL22 promotes Th2 and memory T cell trafficking (D'Ambrosio et al., 2002). Induction of CCL22 further plays a major role in the pathogenesis of allergy, and high levels are detectable in the lung and the skin in asthma and atopic dermatitis, respectively (Romagnani, 2002). In these diseases, CCL22 attracts activated CCR4-positive Th2 cells that maintain the allergic process.

In the absence of inflammation, the receptor CCR4 is expressed predominantly by regulatory T cells (T reg; Iellem et al., 2001), and CCL22 serves as an important factor for the induction of T reg migration in vitro and in vivo (Iellem et al., 2001; Sather et al., 2007). In pancreatic islets, for instance, CCL22 recruits T

[1]Center of Integrated Protein Science Munich, Division of Clinical Pharmacology, University Hospital, Ludwig-Maximilians-Universität München, Munich, Germany; [2]German Cancer Consortium (DKTK), partner site Munich, Munich, Germany; [3]Department of Medicine II, University Hospital, Ludwig-Maximilians-Universität München, Munich, Germany; [4]Institute for Medical Microbiology, Immunology and Hygiene, Technical University of Munich, Munich, Germany; [5]School of Pharmaceutical Sciences, University of Geneva, University of Lausanne, Geneva, Switzerland; [6]Department of Anaesthetics, Pharmacology, Intensive Care and Emergencies, Faculty of Medicine, University of Geneva, Geneva, Switzerland; [7]Department of Immunology, Harvard Medical School, Boston, MA; [8]The Ragon Institute of Massachusetts General Hospital, Massachusetts Institute of Technology, and Harvard, Boston, MA.

Correspondence to Stefan Endres: endres@lmu.de; Ulrich H. von Andrian: uva@hms.harvard.edu.

reg and thus delays diabetes (Montane et al., 2011). In cancer, expression of CCL22 is induced in the tumor tissue of many human malignancies and is thought to mediate T reg immigration through CCR4 into the tumor tissue, leading to an inhibition of antitumor immunity (Curiel et al., 2004; Sugiyama et al., 2013).

In the lymph node, CCL22 is expressed in large amounts by DCs (Tang and Cyster, 1999); however, the function and role of this central CCL22 expression was so far not known. We demonstrate here that CCL22 expression by DCs induces cellular contacts with T regs through their CCR4 receptor. The formation of a cell contact and the interaction with the DCs is a requirement for the suppression of adaptive immunity through T regs (Tang et al., 2006; Onishi et al., 2008; Wing et al., 2008; Sakaguchi et al., 2009). In the present study, we show that deficiency of CCL22 results in a reduction of DC–T reg contacts and in a defect of T reg–mediated suppression, as indicated by an unusually potent adaptive immune response upon vaccination, prolonged survival upon tumor vaccination, and increased susceptibility to inflammatory bowel disease.

Results

DCs are the exclusive source of homeostatic CCL22 in the lymph node

To quantify the protein expression level of homeostatic CCL22 in different murine organs, tissue lysates were analyzed by ELISA. As expected, the highest expression by far of constitutive CCL22 was observed in the lymph node and the thymus. Moderate CCL22 levels were found in the Peyer's patches, the spleen, the lung, the colon, and the skin, and only minimal expression was seen in all other organs and the serum (Fig. 1 A, left). A relatively high amount of CCL22-expressing cells in lymph nodes was confirmed by immunohistochemistry (Fig. 1 A, right). Spontaneous and thus constitutive CCL22 secretion was also observed in vitro: murine splenocytes were cultured without any stimulation, and CCL22 levels were determined in the supernatant at different time points by ELISA. CCL22 secretion was detectable after 12 h, followed by a strong spontaneous secretion during the next 5 d (Fig. 1 B). To confirm the cellular source of constitutive CCL22 expression in the lymph node, we analyzed its expression by DCs, as these cells are known as major CCL22 producers upon stimulation (Vulcano et al., 2001). Indeed, quantitative PCR analysis of freshly isolated lymph node CD11c$^+$ cells revealed high CCL22 mRNA levels, whereas no CCL22 mRNA was found in the CD11c-depleted fraction (Fig. 1 C). The same pattern was observed in the spleen, although CCL22 levels were considerably lower than in the lymph node. Within the different DC subtypes, in particular CD103$^+$ DCs express CCL22, whereas only low levels were detectable on CD11b$^+$ or B220$^+$ plasmacytoid DCs (Fig. 1 D).

Further, higher levels were seen in CD8$^+$CD11b^{neg} so-called lymphoid DCs. Interestingly, DCs in intestinal lymph nodes expressed twofold higher levels of CCL22 than did those within skin-draining lymph nodes (Fig. 1 E). This is consistent with previous data comparing chemokine expression profiles in splenic and lymph node DCs (Vitali et al., 2012; Hao et al., 2016) and fits with transcriptional data from the ImmGen database. In vitro, CCL22 is secreted by both CD11c$^+$ DCs that are obtained from freshly isolated lymphoid tissue and by bone marrow–derived DCs (BMDCs) that are generated by culture in the presence of IL-4 and GM-CSF. Notably, stimulation of both types of DCs by CpG as activator of Toll-like receptor 9 strongly enhanced CCL22 secretion (Fig. 1 F). Taken together, these data show that DCs are the exclusive producers of constitutive CCL22 in the lymph node and the spleen under steady state conditions.

Next, we aimed to determine the cell types responding to CCL22 under homeostatic conditions. The only receptor known so far for CCL22 is CCR4 (Imai et al., 1998). In freshly isolated naive splenocytes, we detected CCR4 expression predominantly by CD4$^+$Foxp3$^+$ T regs and, within those, particularly in memory T regs (Fig. S1 A), which is in accordance with previous reports (Iellem et al., 2001). Further, within unstimulated leukocytes, CCL22 selectively attracted Foxp3$^+$ T regs in a standard migration assay (Fig. S1 B). In conclusion, under homeostatic conditions, CCL22 in the lymph node is expressed exclusively by DCs, and the responder cells carrying the cognate receptor CCR4 are T regs.

CCL22 mediates DC–T reg contacts in vitro and in vivo

It is well established that DC–T reg contacts are critically important for immune regulation by T regs (Tang et al., 2006; Onishi et al., 2008; Wing et al., 2008; Sakaguchi et al., 2009). We hypothesized that DC-derived homeostatic CCL22 attracts T regs to establish DC–T reg contacts. To address this question, we used DCs derived from CCL22-deficient mice. The so far uncharacterized *Ccl22*$^{-/-}$ mouse was recently generated by the National Institutes of Health (NIH) Knockout Mouse Project. As expected, no CCL22 protein was detectable in any of the analyzed tissues of *Ccl22*$^{-/-}$ mice, and no CCL22 secretion was observed in vitro (Fig. S2, A and B). Further, no obvious phenotypical differences were observed compared with WT mice in terms of weight and morphology of lymphoid organs, as well as for the proportion of immune cell subsets (data not shown). We generated BMDCs from WT and *Ccl22*$^{-/-}$ mice and used the supernatants as chemoattractants in a standard migration assay with splenocytes as responder cells. Medium from WT DCs induced specific T reg migration, which was abolished in medium from *Ccl22*$^{-/-}$ DCs (Fig. S3 A).

Next, we isolated CD11c$^+$ DCs from *Ccl22*$^{-/-}$ and WT mice, pulsed them with the OVA$_{323–339}$ peptide, and cocultured them with antigen-specific red-labeled T regs (CD3$^+$CD4$^+$CD25$^+$) and green-labeled conventional CD4 T cells (T convs; CD3$^+$CD4$^+$CD25^{neg}) derived from OT-II transgenic mice. As previously described, when a mixture of T regs and T convs at a 1:1 ratio is used in this assay, T regs outcompete T convs for space on the DCs (Onishi et al., 2008). Indeed, we detected on average three times more T regs than T convs on the surface of WT DCs, while the overall number of T cells in contact with the DCs remained unchanged (Fig. 2 A). In striking contrast, equal numbers of T regs and T convs were observed when *Ccl22*$^{-/-}$ DCs were used. These findings suggest that the dominance of T regs over T convs in terms of interaction with the DCs depends on DC-derived CCL22.

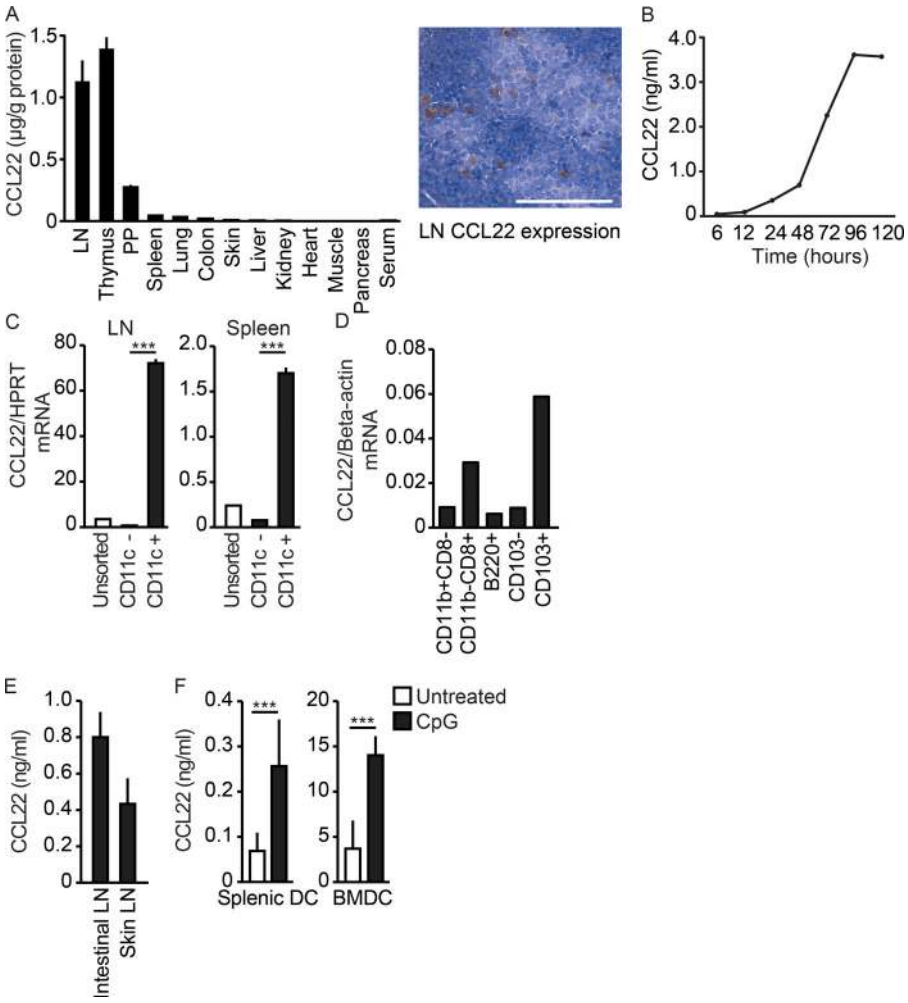

Figure 1. **CCL22 is constitutively expressed in vivo and in vitro. (A)** CCL22 protein was quantified in tissue homogenates and in the serum of BALB/c mice by ELISA (n = 5 mice) and detected by immunohistochemistry in the lymph node (LN). PP, Peyer's patches. Bar, 100 µm. **(B)** 10^6 freshly isolated lymph node cells and splenocytes from C57BL/6 mice were cultured, and CCL22 levels in the supernatants were determined at different time points by ELISA. **(C)** CCL22 mRNA expression from unsorted, CD11c-depleted ($CD11c^-$), or CD11c-enriched ($CD11c^+$) murine lymph node cells or splenocytes was determined by quantitative real-time PCR. **(D)** $CD11b^+CD8^{neg}$, $CD11b^{neg}CD8^+$, $B220^+$, $CD103^+$, and $CD103^{neg}$ cells were sorted from CD11c-enriched splenocytes, and RNA was isolated followed by quantitative real-time PCR. **(E)** CCL22 protein level in intestinal or skin-draining lymph node tissue homogenates of C57BL/6 mice measured by ELISA (n = 3 mice). **(F)** 10^5 freshly isolated $CD11c^+$ splenic DCs or 7-d differentiated BMDCs from C57BL/6 mice were cultured with or without 3 µg/ml CpG for 4 h, and CCL22 levels in the supernatants were determined by ELISA. Data are presented as mean ± SEM and are representative of two to four independent experiments (n = 3–5 mice per group). ***, $P < 0.001$ (two-sided Student's t test).

To further assess the role of CCL22 in the interaction of DCs with T regs, we set up a three-dimensional (3D) assay using a collagen gel matrix with live-cell imaging by confocal laser microscopy. Both DCs and T cells moved in the gel, with more rapid movements observed for T cells. In a typical assay with T cells and DCs, ∼50% of the cells were motile, with an average velocity up to 2.6 µm/min (Video 1). Contacts between DCs and T cells were observed frequently, with a mean duration of 22 min. We embedded red dye–labeled naive WT T regs or T convs with green dye-labeled DCs from either *Ccl22*$^{-/-}$ or WT mice in the collagen matrix and quantified DC–T cell contacts. CCL22-deficient DCs established significantly less contacts with T regs, whereas no difference was observed with T convs (Fig. 2 B and Videos 2, 3, 4, and 5). Similar results were obtained by knocking down CCL22 in WT DCs with CCL22 siRNA (Figs. 2 C and S3 B).

We next analyzed the effects of CCL22 overexpression on DC–T reg contacts. For this purpose, we used a myc- and raf-immortalized DC cell line (Shen et al., 1997) transduced with a lentiviral construct containing CCL22 downstream of a Tet-responsive element and rtTA under the control of a CMV promoter. These cells (DC2.4-CCL22^{dox}) were unable to produce CCL22 even in the presence of T cells, but CCL22 was strongly inducible by addition of doxycycline (Fig. S3 C). We then mixed DC2.4-CCL22^{dox} cells with T regs or T convs in a collagen gel in the presence or absence of doxycycline. As expected, treatment of DC2.4-CCL22^{dox} cells with doxycycline induced CCL22 secretion by DCs (Fig. S3 C) and increased the frequency of DCs in contact with T regs, whereas no increase was seen for DCs and T convs (Fig. 2 D and Videos 6, 7, 8, and 9). To demonstrate that the CCL22-induced DC–T reg contacts are mediated by CCR4 on T regs, we repeated the assay with T regs from CCR4-deficient mice. Indeed, CCR4-deficient T regs did not enhance their contact frequency with DCs upon doxycycline-induced up-regulation of CCL22, indicating that CCL22–CCR4 interaction is required for this process (Fig. S3 D).

To demonstrate that CCL22 is important for DC–T reg contacts in vivo, we imaged the interaction of both cells in the lymph node by two-photon intravital microscopy: $OVA_{323–339}$ peptide-pulsed CCL22-deficient and CCL22-expressing DCs labeled with different dyes were injected into the footpad of transgenic OT-II-Foxp3-GFP mice in which $CD4^+$ T cells recognize the OVA peptide and T regs express GFP. The footpad-draining popliteal lymph node was then imaged by two-photon microscopy, and DC–T reg contacts were quantified (Video 10). Indeed, CCL22-expressing DCs formed significantly more and longer contacts with T regs than CCL22-deficient DCs (Fig. 2 E). The distribution of either DC population in the T cell zones of the draining lymph node was similar, as was their instantaneous velocity.

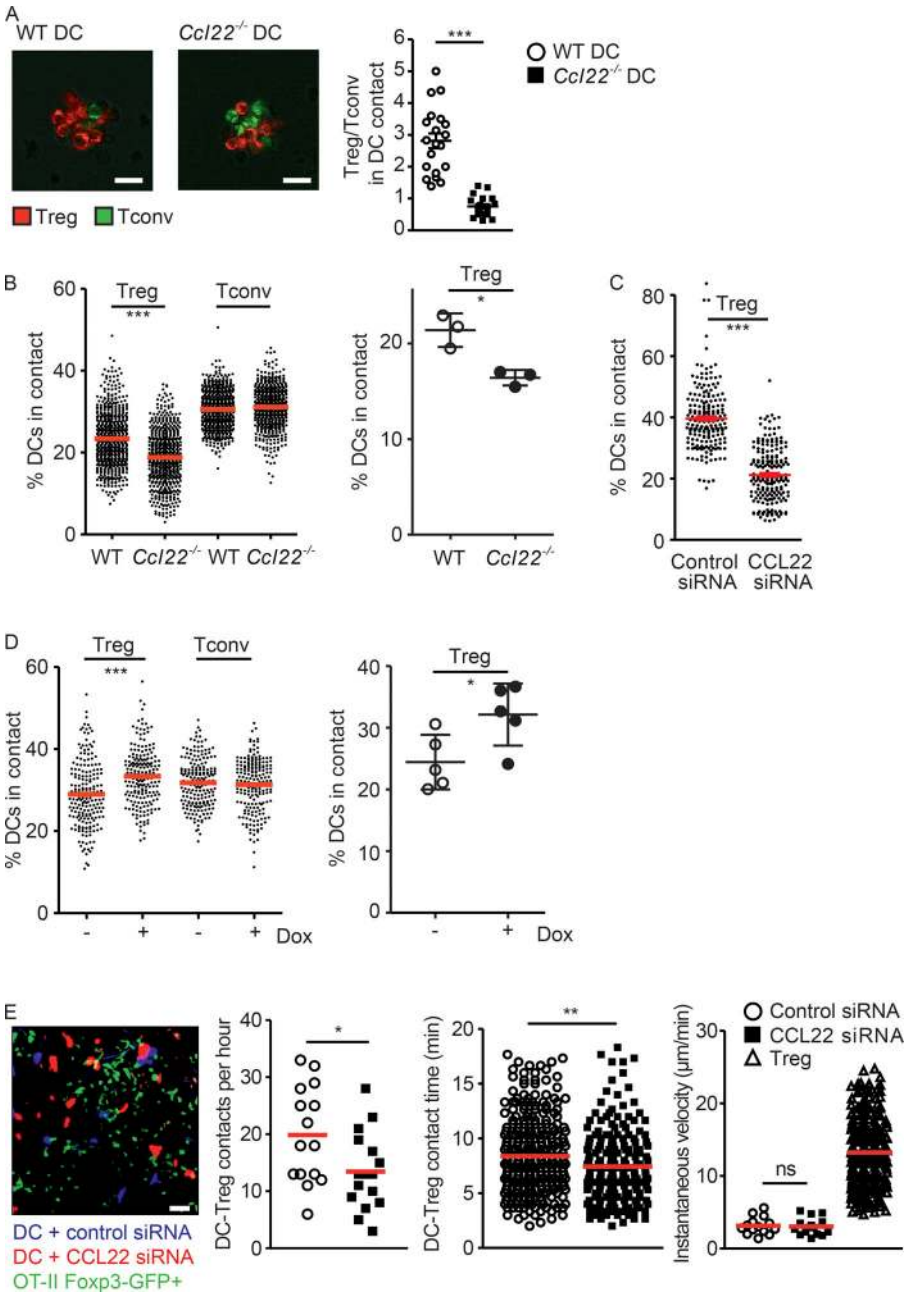

Figure 2. **CCL22 mediates DC–T reg contacts. (A)** T convs (green) and T regs (red) from OT-II mice were mixed at a 1:1 ratio and cultured with unlabeled *Ccl22*$^{-/-}$ or C57BL/6 WT CD11c^{+} splenic DCs in the presence of 1 µg/ml $OVA_{323–339}$ peptide. After 12 h, cells were imaged by confocal microscopy (representative images are shown; bars, 15 µm), and the ratio of T regs to T convs per DC cluster was determined. **(B)** 10^6 T convs or T regs (both red) from C57BL/6 mice were mixed in a collagen gel with 10^5 BMDCs (green) from *Ccl22*$^{-/-}$ or WT mice, and DC–T cell interaction was analyzed by confocal microscopy over 8 h. Resulting videos were analyzed for DC–T cell contacts by a computer algorithm. Left: One dot represents the percentage of DCs in contact with T cells at one time point. Right: Triplicates of the respective conditions were cocultured in parallel. One dot represents the mean percentage of DCs in contact with T cells over the total culture time. **(C)** BMDCs were treated with either control or CCL22 siRNA and, as in B, mixed with T regs, and DC–T cell interaction was quantified. **(D)** DC–T cell interaction was analyzed and depicted as in B, and DC2.4-CCL22^{dox} cells in which CCL22 is inducible by doxycycline (Dox) were used. **(E)** Differently labeled $OVA_{323–339}$-pulsed BMDCs were pretreated with control or CCL22 siRNA 18 h before injection into the footpad of OT-II-Foxp3-GFP mice. The footpad-draining lymph node was imaged by two-photon microscopy (a representative image of a 1-h video is shown; bar, 30 µm), and the number of OT-II-Foxp3^{+}–T reg contacts with DCs per hour as well as the contact time for each T reg–DC contact was quantified by two blinded independent investigators. 15 control DCs and 16 CCL22 knockdown DCs were examined. The instantaneous velocities were calculated from manually tracked cells using Imaris. All in vitro data are representative of three and all in vivo data of two independent experiments. Data are shown as mean ± SEM. *, P < 0.05; **, P < 0.01; ***, P < 0.001; ns, not significant (two-sided Student's *t* test).

Taken together, these data show that homeostatic expression of CCL22 by DCs mediates the formation of DC–T reg contacts that are known to be critical for T reg function.

Vaccination leads to excessive T cell immunity in Ccl22$^{-/-}$ mice

Less DC–T reg interaction should alter T reg function. As in vivo suppression by T regs can be assessed by the extent of a defined T cell immune response, *Ccl22*$^{-/-}$ and WT mice were vaccinated with OVA. Strikingly, OVA-specific cytotoxic T cells (CTLs) were on average more than doubled in *Ccl22*$^{-/-}$ mice compared with WT mice, and 2.7-fold more IFN-γ–positive CTLs were detectable upon in vitro restimulation (Fig. 3, A and B). Indeed, in some *Ccl22*$^{-/-}$ mice, up to 23% of antigen-specific CD8 T cells were observed. Similar findings were observed for CD4^{+} OVA-specific T cells (Fig. S3 E). Thus, deficiency of CCL22 strongly enhances the T cell response upon immunization, supporting the concept of reduced T reg suppression. Interestingly, no difference in the amount of OVA-specific antibodies was detected in *Ccl22*$^{-/-}$ and WT mice upon vaccination, indicating that the humoral response may not be regulated by CCL22 (data not shown).

Ccl22$^{-/-}$ DCs induce stronger adaptive immune responses

We next wanted to provide evidence that the strong immune response in *Ccl22*$^{-/-}$ mice was indeed due to CCL22 deficiency in the DCs. Toward this aim, we vaccinated C57BL/6 WT mice with either WT or *Ccl22*$^{-/-}$ DCs that were pulsed with $OVA_{257–264}$ peptide and quantified T cell immunity. Mice were injected with peptide-pulsed DCs every second week, and 1 wk after the third immunization, the frequency of $OVA_{257–264}$-specific T cells and the extent of the IFN-γ response upon in vitro restimulation

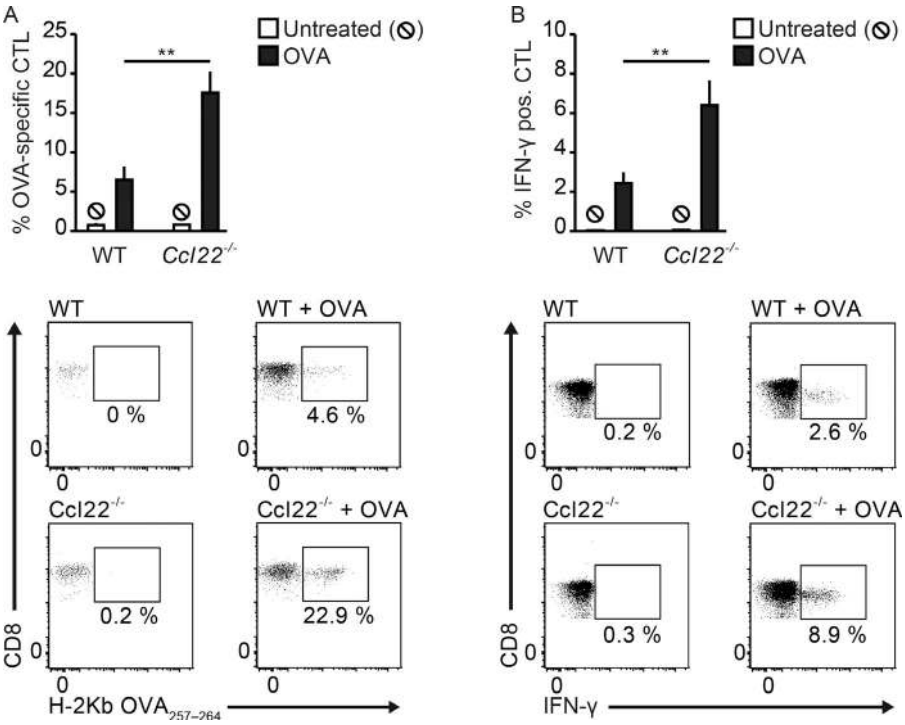

Figure 3. ***Ccl22*$^{-/-}$ mice have excessive T cell responses upon vaccination.** *Ccl22*$^{-/-}$ and WT C57BL/6 mice were injected with OVA protein two times at a 7-d interval, and CpG together with Alum were used as adjuvant. **(A and B)** 1 wk after the last injection, the frequency of OVA-specific cytotoxic T cells ($CD19^{neg}CD3^{+}CD8^{+}$) in the peripheral blood was determined by pentamer (H-2Kb $OVA_{257–264}$) staining (A) and intracellular IFN-γ staining (B) upon restimulation with $OVA_{257–264}$ peptide (n = 11 mice per group treated with OVA and n = 4 mice per group without treatment). Data are shown as mean ± SEM and are pooled from two independent experiments. In total, three experiments with similar results were performed. **, P < 0.01 (two-sided Student's t test).

were quantified. Strikingly, vaccination of WT mice with DCs derived from *Ccl22*$^{-/-}$ mice induced substantially stronger T cell immune responses compared with WT DCs: the frequency of antigen-specific and IFN-γ–positive T cells was more than doubled in mice treated with *Ccl22*$^{-/-}$ DCs (Fig. 4 A). Interestingly, DCs from *Ccl22*$^{-/-}$ mice did not show any differences from WT DCs in terms of in vivo migration, survival, costimulatory molecule expression, or antigen-presentation potential as well as cross-presentation (Fig. S4, A–C). Further, the secretion of proinflammatory cytokines was not altered in *Ccl22*$^{-/-}$ DCs (Fig. S4 D). These findings indicate that the CCL22 production by DCs is important for limiting immune responses against non-self-antigens. To assess the contribution of CCR4 to CCL22-mediated immune regulation, we immunized CCR4-deficient (*Ccr4*$^{-/-}$) mice with $OVA_{257–264}$-pulsed *Ccl22*$^{-/-}$ or WT DCs and quantified T cell immunity. Interestingly, the dominance of *Ccl22*$^{-/-}$ over WT DCs in terms of T cell immune response induction was lost in CCR4-deficient mice, demonstrating that CCL22 regulates T cell immunity through CCR4 (Fig. 4 B). Finally, it was remarkable that the immune responses were generally stronger in CCR4-deficient mice, which is in line with our hypothesis that the CCL22–CCR4 axis regulates T cell immunity.

Ccl22$^{-/-}$ mice show prolonged survival upon vaccination

T regs are critically involved in regulating the immune response against tumors. In the lymph node, T regs inhibit the initiation of an antitumor immune response, and in the tumor tissue, they locally suppress the infiltrating effector T cells (Zou, 2006). To investigate the antitumor immune response in CCL22-deficient mice, we induced subcutaneous tumors that express the OVA antigen (Panc02-OVA-tumors). Mice were vaccinated with OVA protein 1 wk after tumor induction. In *Ccl22*$^{-/-}$ mice, we

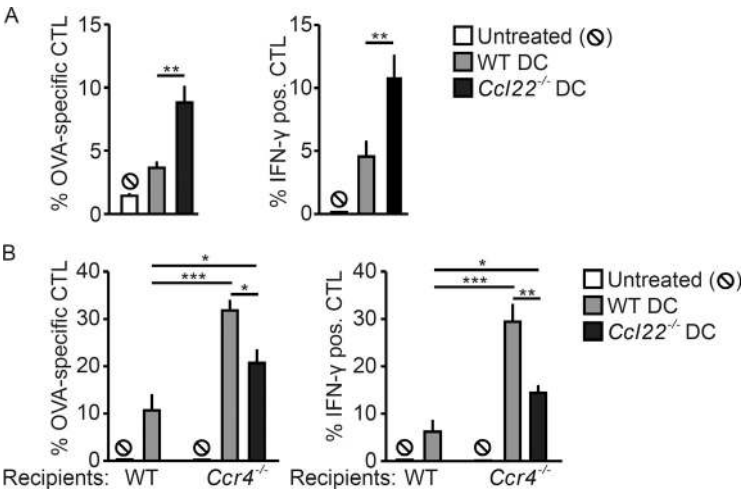

Figure 4. **CCL22-deficient DCs strongly increase T cell immunity. (A)** $OVA_{257–264}$-pulsed *Ccl22*$^{-/-}$ or WT DCs were injected into C57BL/6 WT mice three times every 14 d, and CpG together with Alum were used as adjuvant (n = 15 mice per group injected with DCs and n = 4 mice without treatment). The frequency of splenic OVA-specific cytotoxic T cells was determined by pentamer (left) and intracellular IFN-γ staining (right) as described in Fig. 3 1 wk after the last injection. Data are shown as mean ± SEM and are pooled from two independent experiments. In total, four experiments with similar results were performed. **(B)** $OVA_{257–264}$-pulsed *Ccl22*$^{-/-}$ or WT DCs were injected into either *Ccr4*$^{-/-}$ or WT recipient mice. The experiment was performed as described in A (n = 7 mice per group injected with DCs and n = 2 mice per group without treatment). Data are shown as mean ± SEM and are representative of two independent experiments. *, P < 0.05; **, P < 0.01; ***, P < 0.001 (two-sided Student's t test).

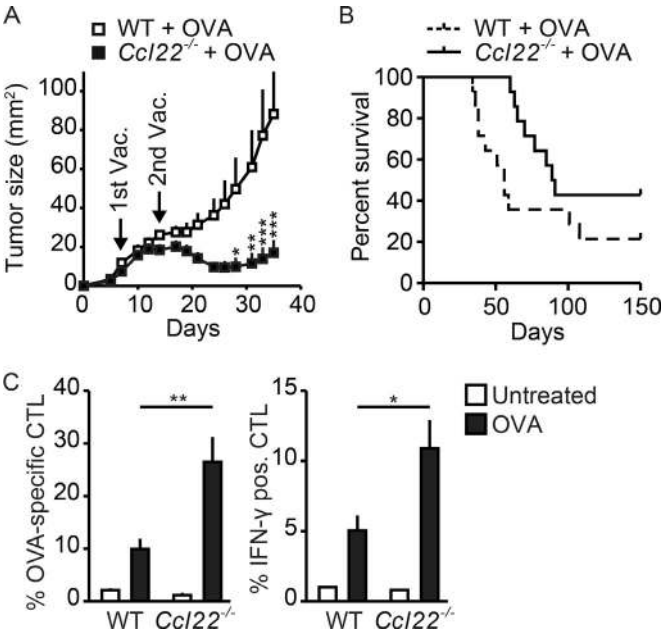

Figure 5. **Vaccination against tumors is more efficient in *Ccl22*$^{-/-}$ mice. (A and B)** *Ccl22*$^{-/-}$ and WT C57BL/6 mice were injected subcutaneously with Panc02-OVA tumors. 1 wk after tumor induction, mice were vaccinated twice with OVA at a 7-d interval as described in Fig. 3, and tumor size as well as survival was monitored (n = 14 mice per group). Growth curves are depicted up to the time point of >20% deaths in one group. Data are shown as mean ± SEM and are pooled from two independent experiments. In total three experiments with similar results were performed. **(C)** 1 wk after the last vaccination, OVA-specific T cells in the peripheral blood of the mice (n = 8, one of three experiments with similar results) were determined as described in Fig. 3. Data are shown as mean ± SE. *, P < 0.05; **, P < 0.01; ***, P < 0.001 (two-sided Student's t test and two-way ANOVA).

observed a significant reduction of tumor growth (Fig. 5 A) and increased survival compared with vaccinated WT mice (Fig. 5 B). A strongly increased OVA-specific T cell response was further observed in tumor-bearing *Ccl22*$^{-/-}$ mice compared with the WT animals (Fig. 5 C). CCL22 was highly expressed in the tumor tissue of WT mice but was undetectable in *Ccl22*$^{-/-}$ mice, indicating that intratumoral CCL22 was secreted uniquely by host-derived tumor-infiltrating cells (Fig. S5 A). Surprisingly, the percentage of intratumoral T regs was not significantly lower in *Ccl22*$^{-/-}$ mice, indicating that tumor rejection is not a consequence of reduced T reg infiltration and that other factors than CCL22 promote T reg infiltration in this model (Fig. S5 B). In addition, lymphocyte subpopulations and proliferation of cytotoxic T cells in terms of Ki67 expression in tumor and lymph nodes were not altered in *Ccl22*$^{-/-}$ mice, suggesting that T cell activation rather than quantity is enhanced by CCL22 deficiency (Fig. S5 B; data on Ki67 expression not shown). In conclusion, CCL22 regulates antitumor immunity, most likely by inhibiting T cell priming in the lymph node.

CCL22-deficient mice are more susceptible to inflammatory bowel disease

We finally aimed to examine whether CCL22-dependent immune regulation also controls inflammatory processes. We chose the dextran sodium sulfate (DSS)–induced colitis model in which bowel inflammation is induced by innate immune activation but is controlled by T regs (Boehm et al., 2012). When mice were fed with the standard dose of 2% DSS, both *Ccl22*$^{-/-}$ and WT mice developed severe colitis (data not shown). We next used a DSS concentration of 0.5% that was insufficient to induce colitis in WT mice. Strikingly, whereas WT mice did not show any signs of colitis, *Ccl22*$^{-/-}$ mice were still severely affected by the disease. This was determined by the clinical disease activity score composed of weight loss, diarrhea, and the detection of blood in the stool, as well as by scoring mucosal destruction and leukocyte infiltration and by inflammation-induced reduction of the colon length (Fig. 6, A–D). In conclusion, *Ccl22*$^{-/-}$ mice are more susceptible to DSS-induced colitis, suggesting that CCL22 may be critically involved in the prevention of inflammatory diseases.

Discussion

Constitutively expressed chemokines have essential roles in the organism, and most of them, such as CCL21 or CXCL12, have been characterized in detail for their specific functions (Förster et al., 1999; Schajnovitz et al., 2011). The functional role of CCL22 expression in lymphoid organs has so far been unknown, although its strong constitutive expression in the lymph node and the thymus has been described previously (Schaniel et al., 1998; Tang and Cyster, 1999). We show here that CCL22 expression by DCs in secondary lymphoid organs serves as a mediator for DC–T reg contacts that are crucial for immune regulation by T regs. As a functional consequence of CCL22 deficiency, we found overwhelming T cell immunity upon vaccination, enhanced responses against tumors, and stronger inflammatory responses.

Under steady state conditions in the lymph node, CCL22 is expressed at high levels exclusively by DCs, and the corresponding receptor, CCR4, is expressed specifically by T regs. Interestingly, CCL22 expression was predominantly seen in CD103^{+} and CD11b^{-}CD8^{+} DCs, which are both known for their potential to induce tolerance, further suggesting a role for immune regulation (Merad et al., 2013). One could speculate on other functional consequences, beyond induction of DC–T reg contacts, of this distinct chemokine and cognate chemokine receptor expression: T regs could be attracted to lymphoid tissues via the CCL22–CCR4 axis; however, we found that in *Ccl22*$^{-/-}$ mice, homing of T regs to the lymph node or the spleen was not altered. Further, in *Ccl22*$^{-/-}$ mice, T regs were regularly located in the T cell areas with no difference from WT mice (data not shown). It is known that T regs use other receptors, such as CCR7 (Schneider et al., 2007), to enter the lymph node, although synergy of chemokine receptors can be required for efficient organ homing (Scimone et al., 2004; Halin et al., 2005). However, in a mixed bone marrow chimeric mouse with a WT and a CCR4-deficient donor, no disadvantage of CCR4-deficient T regs was observed in terms of homing to the spleen or the lymph node (Sather et al., 2007). Taken together, these data show that CCL22-CCR4 interaction seems to be dispensable for homing of T regs to the lymph nodes.

Beside their function in mediating tissue immigration, chemokines can also act locally to establish cell–cell interactions

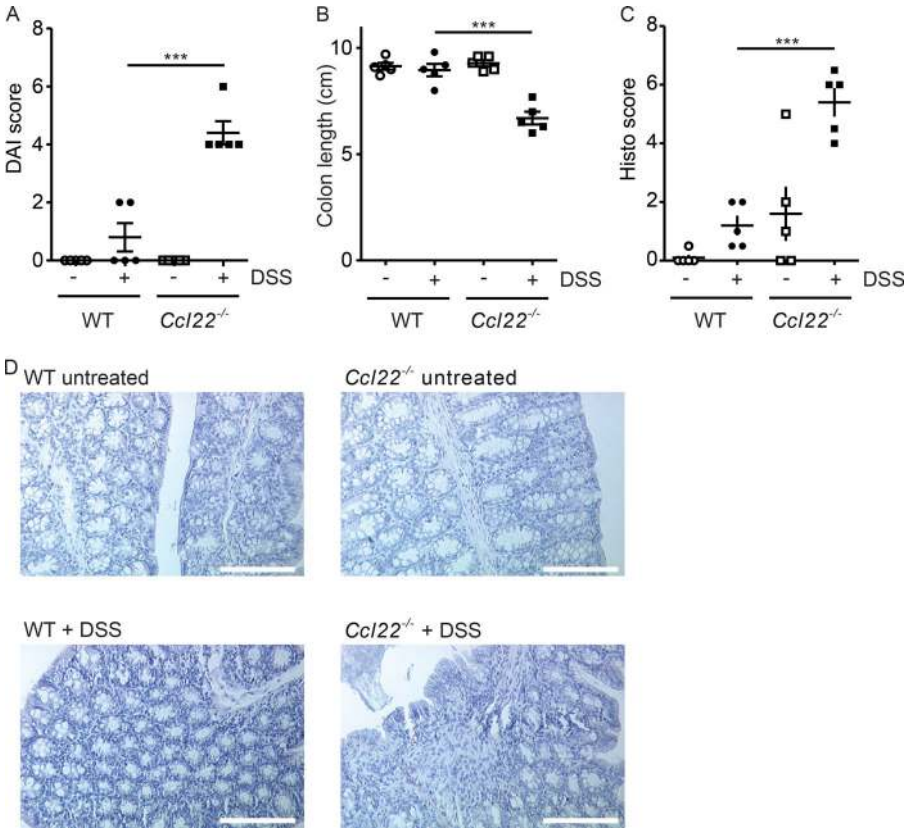

Figure 6. ***Ccl22*-deficient mice are highly susceptible to DSS-induced colitis.** *Ccl22*$^{-/-}$ and WT C57BL/6 mice were fed with or without 0.5% DSS dissolved in tap water over a period of 1 wk followed by 1 wk of recreation, in three consecutive cycles. Disease severity was analyzed at day 7 after the last cycle of DSS administration. **(A)** Loss of body weight, diarrhea, and the presence of occult or overt blood in the stool was used to determine the clinical disease activity index (DAI). **(B–D)** The colon length was measured (B) and tissue sections of the colon were analyzed for mononuclear and neutrophilic cell infiltration, crypt hyperplasia, epithelial injury, and crypt abscesses (C and D) to determine the histological score (bars, 200 µm). Data are shown as mean ± SEM of five mice per group and are representative of three independent experiments. ***, P < 0.001 (two-sided Student's *t* test).

(Wu et al., 2001; Castellino et al., 2006; Rapp et al., 2015). We demonstrate here that CCL22 secretion by DCs indeed induces the formation of cell contacts with T regs in vitro and in vivo. Importantly, this cellular interaction was dependent on CCR4 expression by T regs and was not seen for other T cells. We further show that CCL22 is required for T regs to outcompete T effector cells for space around the DCs, a process that is important for suppression by T regs (Tadokoro et al., 2006; Onishi et al., 2008). In general, cellular interaction of T regs with DCs is crucial for the immunosuppressive function of T regs (Misra et al., 2004; Tang et al., 2006; Onishi et al., 2008; Wing et al., 2008; Sakaguchi et al., 2009). In consequence, a selective deficiency of CCL22 in DCs strongly enhanced immunity upon vaccination, reflected by a more than twofold higher frequency of antigen-specific CD8$^+$ T cells. Thus, constitutive CCL22 expression by DCs regulates the adaptive immune response, most likely through the induction of DC–T reg contacts.

We could show here that the CCL22-induced formation of DC–T reg contacts and the resulting strong induction of T cell immunity are dependent on CCR4 expression by T regs. Interestingly, whereas no direct phenotype can be seen in *Ccr4*$^{-/-}$ mice, severe autoimmunity occurs when CCR4 is selectively absent on Foxp3$^+$ T regs (Sather et al., 2007). Further, CCR4-deficient T regs fail to protect *Rag2*$^{-/-}$ recipient mice from CD4$^+$CD25$^-$CD45RB^{high} T cell transfer colitis (Yuan et al., 2007), and CCR4 antagonists can diminish T reg function (Bayry et al., 2008; Pere et al., 2011). We demonstrate here that *Ccl22*$^{-/-}$ mice are markedly more susceptible to DSS-induced colitis, and as T regs control disease activity in this model (Boehm et al., 2012), we predict that reduced CCL22-dependent DC–T reg interaction enhances inflammation. Although a key contribution of CCL22–CCR4 interaction in immune regulation by T regs seems unquestionable, it remains unclear why *Ccl22*$^{-/-}$ and *Ccr4*$^{-/-}$ mice display no spontaneous autoimmunity. This needs further careful observation and may also be influenced by age, genetic background, or even the microbiome. In addition, other factors, such as CCR5 or CCR7 ligands, can also induce T cell and thus T reg migration and may partially substitute for CCL22 deficiency. Further, contacts with DCs can be stabilized through T cell receptor signaling on T regs (Levine et al., 2014). Thus, under steady state conditions, deficiency of CCL22 may be compensated for by other factors that appear, however, not to be sufficient to prevent autoimmunity in the presence of appropriate triggers. Here, it will also be interesting to analyze the regulation process of CCL22 expression itself in the presence of different triggers, such as Toll-like receptor stimulation, e.g., in infection or autoimmune disease. Taken together, our data show that expression of CCL22 by DCs contributes to T reg–mediated immune suppression and prevents inflammatory immune responses.

In consideration of the crucial role of CCL22 in immune regulation, an important question is whether CCL17, the second ligand for CCR4, exerts similar functions. Intriguingly, however, in *Ccl17*$^{-/-}$ mice, DSS-induced colitis was strongly attenuated and *Ccl17*$^{-/-}$/*Rag-1*$^{-/-}$ mice were even protected from T cell (CD45RB^{high}) transfer-induced colitis (Heiseke et al., 2012). A functionally different role of both chemokines was further seen in models of cardiac allograft transplantation: whereas allograft survival in *Ccr4*$^{-/-}$ mice was decreased (Lee et al., 2005), it was

increased in *Ccl17*$^{-/-}$ mice (Alferink et al., 2003), indicating that CCL17 rather promotes the immune response. Thus, although the chemokines CCL17 and CCL22 are structurally related, their mode of action is different. Homeostatic CCL17 expression in secondary lymphoid organs exists, but we show here that it is 10-fold lower compared with CCL22 (Fig. S2 A). In addition, the receptor CCR4 binds with a threefold lower affinity to CCL17 than to CCL22 (Imai et al., 1998). Thus, we conclude that CCL17 does not substantially act on T regs, at least not in lymph nodes under homeostatic conditions. Moreover, using CCL17-deficient cells, it has been shown that CCL17 boosts LPS-induced proinflammatory cytokine production in an autocrine manner through direct action on the CCR4 receptor of DCs (Heiseke et al., 2012). Using CCL22-deficient DCs, we did in contrast not detect any effects of CCL22 on cytokine production (Fig. S4 D). These findings may in addition explain the remarkable differences between the two chemokines.

We show here that an exclusive deficiency of CCL22 potently enhances the adaptive immune response induced by vaccination and leads to robust antitumor immune responses. Therapeutic targeting of T regs to enhance the immune response to cancer or infections has been and is subject of numerous studies (Curiel, 2008). This approach is limited by the lack of specific target molecules on T regs (Smigiel et al., 2014) and by the fact that complete elimination of T regs will cause severe autoimmunity (Lahl et al., 2007). As DC–T reg interaction is critical for T reg–mediated suppression, targeting the involved pathways, rather than the T reg itself, represents a promising novel strategy. In studies by Ishida and Ueda (2006), an anti-CCR4 antibody was used to target both CCR4-expressing malignant lymphocytes and T regs, leading to better tumor control. Our data suggest that targeting the CCL22–CCR4 axis could not only deplete T regs but rather inhibit their interaction with DCs, resulting in stronger immunity. Today we have a new class of drugs, the immune checkpoint inhibitors that modulate key pathways in the interaction of T cells with DCs and other target cells and exert powerful immune activation (Pardoll, 2012): Ipilimumab blocks the interaction of CTLA-4 on T regs and T effector cells with CD80 and CD86 on DCs and thus strongly enhances T cell immunity. Blockade of the interaction of PD-1 on T effector cells with PD-L1 on DCs or tumor cells potently activates adaptive immunity. Several PD-1 or PD-L1 blocking antibodies are approved for the treatment of different types of cancer (Brahmer et al., 2015; Larkin et al., 2015). A limitation of the so far available immune checkpoint inhibitors is the induction of autoimmunity. We suggest that the CCL22–CCR4 axis also represents an immune checkpoint and that targeting CCL22 interaction with its receptor could represent a powerful and potentially less harmful therapeutic strategy. In summary, we identified here CCL22 as an important novel regulator of adaptive immunity with impact on vaccine development, host response against cancer, and inflammation.

Material and methods

Mice and cell lines

Female C57BL/6 and BALB/c mice were purchased from Janvier. CCL22 knockout (*Ccl22*$^{-/-}$) mice on the C57BL/6 background were obtained from the NIH-founded Knockout Mouse Project. The CCL22 knockout was achieved by CCL22 gene deletion through homologous recombination using a lacZ neomycin reporter vector. PCR was used to identify homozygous *Ccl22*$^{-/-}$ mice. Mice transgenic for a chicken $OVA_{323–339}$-specific T cell receptor (OT-II) were purchased from the Jackson Laboratory. *Ccr4*$^{-/-}$ mice on the C57BL/6 background were a gift from Anne Krug (Institute of Immunology, Ludwig-Maximilians-Universität München, Munich, Germany). OTII-Foxp3-GFP mice on the C57BL/6 background were a gift from Vijay Kuchroo (Evergrande Center for Immunologic Diseases at Harvard Medical School, Boston, MA). Mice were 5–10 wk of age at the onset of experiments. Transgenic mice bred in-house and C57BL/6 control mice purchased from Janvier were housed together before being used in experiments. Animal studies were approved by the local regulatory agency (Regierung von Oberbayern, Munich, Germany). The OVA-transfected murine pancreatic cancer cell line Panc02-OVA was a gift from Max Schnurr (Division of Clinical Pharmacology, Klinikum der Universität München, Munich, Germany). HEK293T cells were obtained from ATCC, and the murine immortalized DCs line DC2.4 was kindly provided by K. Rock (Department of Pathology, University of Massachusetts, Worcester, MA). Cell lines were authenticated using STR (LGC Standards) and were cultured in complete DMEM or RPMI medium (PAA Laboratories) and routinely tested for mycoplasma contamination by MycoAlert Mycoplasma Detection Kit (Lonza). The DC2.4-CCL22^{dox} cell line was generated by lentiviral transduction with a construct containing a doxycycline-inducible CCL22 expression cassette as described (Bauernfeind et al., 2012). Syngeneic tumors were induced by subcutaneous injection of 0.5 × 10^6 tumor cells into the right flank of C57BL/6 or *Ccl22*$^{-/-}$ mice. The sample size of each experiment was chosen according to previous experience conducting similar experiments. All animal experiments were randomized, and tumor growth was measured by investigators blinded to the group allocation.

Cytokine assays of tissue lysates

Tissue homogenates were resuspended in lysis buffer (Bio-Rad Laboratories) and centrifuged. Total protein concentration was measured by Bradford assay (Bio-Rad Laboratories). All samples were diluted to a protein concentration of 10 mg/ml, and CCL22 or CCL17 was measured by ELISA (R&D Systems). The final cytokine concentration was calculated as nanograms of cytokine per gram of protein in the respective lysate.

Immunohistochemistry

For analysis of CCL22 expression from formalin-fixed, paraffin-embedded murine tissue, 3-µm slices were deparaffinized, rehydrated, and heated in Tris-EDTA buffer, pH 9.0, supplemented with 0.5% Tween-20. CCL22 was detected using a rabbit monoclonal anti-CCL22 antibody (ab124768; Abcam) at a dilution of 1:200. After a 1-h incubation period with a secondary HRP-conjugated anti-rabbit antibody (ab205718; Abcam) at a dilution of 1:2,000, staining was performed using 3,3-diaminobenzidine substrate solution. The slices were counterstained with hematoxylin.

Monoclonal antibodies and flow cytometry

CD3e-APC or CD3e-PE (clone 145-2C11), CD4-APC/Cy7 or CD4-PerCp (clone GK1.5), CD8α-APC/Cy7 or CD8α-PacBlue (clone 53–6.7), CD11c-APC or CD11c-PE (clone N418), CD11b-PerCP (clone M1/70), CD19-PerCP/Cy5.5 (clone HIB19), CCR4-APC or CCR4-PE/Cy7 (clone 2G12), CD25-PE (clone PC61), IFN-γ-Pacific Blue (clone XMG1.2), and Foxp3-Pacific Blue (clone MF-14) were all from BioLegend. T regs were stained with a Foxp3 Staining Buffer Set (eBioscience) according to the manufacturer's instructions. For intracellular IFN-γ staining, peripheral blood or splenocytes were incubated with red blood cell lysis buffer (BD Pharm Lyse; BD Bioscience) for 3 min. Lymphocytes were then stimulated with 100 nM $OVA_{257–264}$ peptide or $OVA_{323–339}$ peptide (both InvivoGen) for 1 h at 37°C before 1 µg/ml brefeldin A (Sigma-Aldrich) was added. After 3 h, cells were surface stained with CD8-APC/Cy7 and CD19-PerCP, then fixed and permeabilized using the Foxp3 Staining Buffer Set (eBioscience) and incubated with an anti–IFN-γ-Pacific Blue antibody. Pentamer staining was performed with H-2Kb $OVA_{257–264}$ R-PE pentamers (ProImmune) according to the manufacturer's instructions. Events were measured on a FACS Canto II flow cytometer (BD Biosciences) and analyzed with FlowJo software (TreeStar).

Cell sorting

CD11c, B220, CD103, CD8, and CD49b splenic and lymph node cell isolation from WT and *Ccl22*$^{-/-}$ mice was performed by one-step magnetic cell sorting (Miltenyi Biotec) or on an Aria II cytometer. $CD4^+CD25^+$ cells and $CD4^+CD25^{neg}$ cells were purified from the spleen and lymph nodes of WT or OT-II mice by two-step magnetic cell sorting (Miltenyi Biotec). Purity of sorted cells was on average >90%.

RNA isolation and quantitative PCR analysis

Total RNA was extracted from sorted and unsorted single-cell suspensions using the High Pure RNA Isolation Kit (Qiagen) according to the manufacturer's instructions. 1 µg of RNA was converted into cDNA using the Revert Aid First Strand cDNA Synthesis Kit (Fermentas). Quantitative real-time PCR amplification was performed with the Light Cycler TaqMan Master (Roche Diagnostics) on a LightCycler 2.0 instrument (Roche Diagnostics) together with the Universal Probe Library System (Roche Diagnostics; CCL22 probe #84, hypoxanthine phosphoribosyltransferase [HPRT] probe #69, β-actin probe #64). Relative gene expression is shown as a ratio of the CCL22 mRNA expression level to the expression level of HPRT or β-actin mRNA. The primers for CCL22 (forward: 5′-TCTTGCTGTGGC AATTCAGA-3′; reverse: 5′-GAGGGTGACGGATGTAGTCC-3′), HPRT (forward: 5′-GGAGCGGTAGCACCTCCT-3′; reverse: 5′-CTGGTTCATCATCGCTAATCAC-3′), and β-actin (forward: 5′-CTAAGGCCAACCGTGAAAAG-3′; reverse: 5′-ACCAGAGGCATA CAGGGACA-3′) were obtained from Metabion.

Generation of BMDCs

Bone marrow cells of WT and *Ccl22*$^{-/-}$ mice were isolated from the femur and tibia bones. After incubation with red blood lysis buffer, cells were diluted to 10^6 cells/ml in RPMI 1640 medium supplemented with 10% FBS (Gibco), 1% L-glutamine, 1 U/ml penicillin, 0.1 mg/ml streptomycin (all PAA), 20 ng/ml GM-CSF, and 20 ng/ml IL-4 (both PeproTech). BMDCs were harvested on day 7.

Chemokine knockdown by siRNA

WT BMDCs were transfected (Amaxa nucleofector system; Y-001 immature DC program) at a cell number of 10×10^6 with 10 ng CCL22 siRNA (Mm_Ccl22_3 FlexiTube siRNA; Qiagen) or control siRNA (AllStars Negative Control siRNA; Qiagen). After transfection, DCs were rested for 2 h.

2D DC–T cell coculture assay

T reg and T conv cells isolated from OT-II mice by magnetic cell sorting were labeled with PKH-26 (red) and PKH-67 (green; both Sigma-Aldrich), respectively, according to the manufacturer's instruction. PKH-labeled T regs and T conv cells were cultured at a 1:1 ratio (5×10^4 each) with unlabeled splenic DCs (5×10^3) in 96-well non-tissue culture round-bottom plates as described before (Onishi et al., 2008). After 6-h culture in the presence of 1 µg/ml $OVA_{323–339}$, cells were gently transferred to a glass-bottomed dish for confocal microscopy. The ratio of T regs to T convs per DC cluster was determined independently in 40 images by three blinded investigators.

3D DC–T cell coculture assay

DC2.4-$CCL22^{dox}$ cells were harvested from stable in vitro cultures, and BMDCs were prepared from the bone marrow of WT or *Ccl22*$^{-/-}$ mice. DC2.4-$CCL22^{dox}$ cells and BMDCs were labeled with PKH-67 (Sigma-Aldrich). T reg and T conv cells were obtained from WT or *Ccr4*$^{-/-}$ mice by magnetic cell sorting and were labeled with PKH-26 (Sigma-Aldrich). Subsequently, 2×10^5 BMDCs or DC2.4-$CCL22^{dox}$ cells and 10^6 T reg or T conv cells were resuspended in a total volume of 100 µl containing 20 µl of a collagen gel master mix solution. To prepare the collagen master mix, 83 µl of 3 mg/ml rat tail collagen type I (Invitrogen), 10 µl M199 medium (Sigma-Aldrich), 2 µl distilled water, 2.1 µl of 1N NaOH, and 2.9 µl of 7.5% sodium bicarbonate were mixed to a total volume of 100 µl. The cell suspension was then placed in a CELLview cell culture dish with glass bottom (Greiner Bio-One) and polymerized to a gel for 45 min at 37°C. For the induction of CCL22 expression, DC2.4-$CCL22^{dox}$ cells were pretreated with 2 µg/ml doxycycline. The gels were then analyzed by confocal microscopy in a live-cell imaging chamber (Leica TCS SP5) at 37°C and 5% CO_2. Cuboids of 500 × 500 × 100 µm within the gel were filmed for 500 min with a lateral and vertical resolution of at least 256 × 256 pixels. Each cuboid consisted of 21 single-slice images with a distance of 5 µm, and images were obtained every 150 s. Recorded slices were transformed to a 3D model in Imaris (Bitplane AG). Videos were analyzed with a customized image-analyzing algorithm (Wimasis Image Analysis) for DC–T cell contacts. Briefly, red and green fluorescence channels were split, followed by a cell division algorithm to split cell clusters into individual cells. The positional information of the cells was then analyzed, and cells were considered to be in contact in case of an overlap of their pixels. For each frame, the percentage of DCs in contact with T cells was calculated.

Two-photon intravital microscopy

BMDCs were prepared from bone marrow of C57BL/6 mice and transfected with either control or CCL22 siRNA. Subsequently, DCs were pulsed with 1 µg/ml $OVA_{323–339}$ peptide and labeled for 20 min at 37°C with 10 mM 5- and 6-([(4-chloromethyl) benzoyl] amino) tetramethylrhodamine (CellTracker CMTMR; Invitrogen) or 7-amino-4-chloromethylcoumarin (Cell Tracker CMAC; Invitrogen). Control siRNA- and CCL22 siRNA-treated DCs (both 10^6) were coinjected in 20 µl IMDM (with 10% FCS) containing 10 ng *Escherichia coli* LPS (Sigma) into the right hind footpad of C57BL/6 OT-II-Foxp3-GFP mice. 18 h after injection of DCs, animals received 100 µg anti-CD62L antibody (Mel-14) to inhibit lymph node homing during imaging, and the right popliteal lymph node was analyzed for 1 h by two-photon intravital imaging with an Olympus BX50WI fluorescence microscope equipped with a 20-fold magnification, 0.95-NA objective (Olympus) as described (Mempel et al., 2004). Image data collection was repeated every 20 s for 1 h. The 4D image dataset was processed using Imaris software (Bitplane) to create sequential 2D maximum-intensity projections. The absolute number of T reg contacts per DC over the time period of 1 h was quantified by individual inspection of each time point. Cellular interactions that were <2 min or incompletely depicted spatially or temporally were excluded from the analysis.

OVA and DC vaccination

For OVA vaccination, mice were injected i.p. with 200 µl PBS containing 50 µg OVA (Sigma-Aldrich), 10 µg CpG 1826 (Coley Pharmaceutical Group), and 2 mg Imject Alum (Thermo Fisher Scientific) at weekly intervals. 1 wk after the second OVA injection, peripheral blood was collected to verify vaccination efficiency. For DC vaccination, BMDCs were generated from WT and *Ccl22*$^{-/-}$ mice, pulsed with 100 nM $OVA_{257–264}$ peptide (InvivoGen), and activated with 6 µg/ml CpG 1826 for 4 h. WT or *Ccr4*$^{-/-}$ mice were injected i.p. with 4×10^5 $OVA_{257–264}$ peptide–pulsed activated BMDCs together with 10 µg CpG 1826 and 2 mg Imject Alum three times every second week. 1 wk after the last injection, peripheral blood or spleens were collected to analyze T cell responses.

Induction of DSS colitis

WT and *Ccl22*$^{-/-}$ mice received DSS dissolved in tap water at a concentration of 0.5% ad libitum for 7 d followed by 7 d of normal tap water. This cycle was repeated three times, and mice were sacrificed at day 42. The disease activity index described by Cooper et al. (1993) including body weight, diarrhea, and the presence of occult or gross blood in the stool was applied to quantify the severity of colitis. Further, the length of the colon was used to determine disease activity. For hematoxylin and eosin staining, paraffin-embedded specimens were cut at 4 µm. The histological score was evaluated as described previously. Briefly, mononuclear inflammation or neutrophilic infiltration, crypt abscesses, crypt hyperplasia, and mucosal injury or ulceration were assessed. Each of the four criteria was graded (0, absent; 1, mild; 2, moderate; 3, severe), and the sum gave the final score.

In vitro migration

Freshly isolated C57BL/6 splenocytes (1×10^6) were put in the upper well of a 96-well Transwell migration plate (pore diameter 5 µm; Corning). 50 ng/ml of recombinant CCL22 (Peprotech) or supernatant from C57BL/6 and *Ccl22*$^{-/-}$ BMDCs cultured for 24 h was used as chemoattractant in the lower chamber. After 4–6 h, the migrated cells were harvested and analyzed by flow cytometry.

In vivo migration

C57BL/6 mice were subcutaneously injected (leg) with 4.25×10^6 CpG-stimulated (6 µg/ml) and eFluor450-stained (5 µM, Cell Proliferation Dye; eBioscience) C57BL/6 or *Ccl22*$^{-/-}$ BMDCs. DC survival, costimulatory molecule expression, and migration into the ipsilateral inguinal lymph node were analyzed using flow cytometry 36 h after injection.

Statistics

All data are presented as mean ± SEM, and the statistical significance of differences was determined by the two-tailed Student's *t* test. Differences in tumor size were analyzed using two-way ANOVA with Bonferroni post hoc test and differences in survival by log-rank test. Statistical analyses were performed using GraphPad Prism 7 (GraphPad Software). P values <0.05 were considered significant.

Online supplemental material

Fig. S1 shows how CCR4 is expressed selectively by T regs. Fig. S2 shows that *Ccl22*$^{-/-}$ mice are deficient for CCL22 but proficient for CCL17 protein. Fig. S3 shows that DC-secreted CCL22 is a strong chemoattractant for T regs, siRNA efficiently knocks down CCL22 in DC, doxycyclin induces CCL22 in DC2.4-$CCL22^{Dox}$ cells, CCL22-induced DC–T reg contacts depend on CCR4 expression by T regs, and that CD4 T cell immunity is enhanced in *Ccl22*$^{-/-}$ mice. Fig. S4 shows that WT and *Ccl22*$^{-/-}$ DCs do not differ in terms of in vivo migration, survival, costimulatory molecule expression, and in vitro cytokine production. Fig. S5 shows that CCL22 is strongly expressed in the tumor tissue of WT mice, but not in *Ccl22*$^{-/-}$ mice, and lymphocyte subpopulations in the tumor and lymph nodes are not altered in *Ccl22*$^{-/-}$ mice. Videos 1–9 show cocultures of DC with T regs in a 3D collagen gel. Video 1 and 2 show WT BMDCs cocultured with T regs. Video 3 shows *Ccl22*$^{-/-}$ BMDCs cocultured with T regs. Video 4 shows WT BMDCs cocultured with T convs. Video 5 shows *Ccl22*$^{-/-}$ BMDCs cocultured with T convs. Video 6 shows DC2.4 cells without doxycycline preincubation (i.e., without CCL22 expression) cocultured with T regs. Video 7 shows DC2.4 cells with doxycycline preincubation (i.e., with CCL22 expression) cocultured with T regs. Video 8 shows DC2.4 cells without doxycycline preincubation (i.e., without CCL22 expression) cocultured with T convs. Video 9 shows DC2.4 cells preincubated with doxycycline (i.e., with CCL22 expression) cocultured with T convs. Video 10 shows two photon in vivo imaging of $OVA_{323–339}$-pulsed BMDCs pretreated with control or CCL22 siRNA in the lymph node of OT-II-Foxp3-GFP mice.

Acknowledgments

We thank Timon E. Adolph and Arthur Kaser (Cambridge, UK) for help in assessing the histology scoring of colitis.

The work was supported by grants from the German Research Foundation (DFG AN 801/2-1 to D. Anz and S. Endres, and DFG GK 1202 to D. Anz, S. Endres, C. Bourquin, W.G. Kunz, D. Lisowski, S. Haubner, S. Moder, S. Eiber, and R. Thaler), Deutsche Krebshilfe (grant 111326 to D. Anz), Sander Stiftung (grant 2016.028.1 to D. Anz), the Swiss National Science Foundation (grants 138284, 156372), the National Center of Competence in Research Bio-Inspired Materials (to C. Bourquin), Oncosuisse (KLS-2910-02-2012 to C. Bourquin), Bundesministerium für Bildung und Forschung (USA 11/A04 to S. Endres) and Elite Network of Bavaria (i-Target: Immunotargeting of cancer to S. Endres, I. Piseddu, B. Meyer and N. Röhrle).

The authors declare no competing financial interests.

Author contributions: Conception and design: M. Rapp, U.H. von Andrian, S. Endres, and D. Anz; development of methodology and acquisition of data: M. Rapp, M.W.M. Wintergerst, W.G. Kunz, V.K. Vetter, M.M.L. Knott, D. Lisowski, S. Haubner, S. Moder, R. Thaler, S. Eiber, B. Meyer, N. Röhrle, I. Piseddu, S. Grassmann, P. Layritz, B. Kühnemuth, S. Stutte, S. Endres, and D. Anz; writing, review, and revision of the manuscript: M. Rapp, C. Bourquin, U.H. von Andrian, S. Endres, and D. Anz.

Submitted: 12 February 2017
Revised: 8 November 2018
Accepted: 1 March 2019

References

Alferink, J., I. Lieberam, W. Reindl, A. Behrens, S. Weiss, N. Hüser, K. Gerauer, R. Ross, A.B. Reske-Kunz, P. Ahmad-Nejad, et al. 2003. Compartmentalized production of CCL17 in vivo: strong inducibility in peripheral dendritic cells contrasts selective absence from the spleen. *J. Exp. Med.* 197:585–599. https://doi.org/10.1084/jem.20021859

Bauernfeind, F., A. Rieger, F.A. Schildberg, P.A. Knolle, J.L. Schmid-Burgk, and V. Hornung. 2012. NLRP3 inflammasome activity is negatively controlled by miR-223. *J. Immunol.* 189:4175–4181. https://doi.org/10.4049/jimmunol.1201516

Bayry, J., E.Z. Tchilian, M.N. Davies, E.K. Forbes, S.J. Draper, S.V. Kaveri, A.V. Hill, M.D. Kazatchkine, P.C. Beverley, D.R. Flower, and D.F. Tough. 2008. In silico identified CCR4 antagonists target regulatory T cells and exert adjuvant activity in vaccination. *Proc. Natl. Acad. Sci. USA.* 105:10221–10226. https://doi.org/10.1073/pnas.0803453105

Boehm, F., M. Martin, R. Kesselring, G. Schiechl, E.K. Geissler, H.J. Schlitt, and S. Fichtner-Feigl. 2012. Deletion of Foxp3+ regulatory T cells in genetically targeted mice supports development of intestinal inflammation. *BMC Gastroenterol.* 12:97. https://doi.org/10.1186/1471-230X-12-97

Brahmer, J., K.L. Reckamp, P. Baas, L. Crinò, W.E. Eberhardt, E. Poddubskaya, S. Antonia, A. Pluzanski, E.E. Vokes, E. Holgado, et al. 2015. Nivolumab versus Docetaxel in Advanced Squamous-Cell Non-Small-Cell Lung Cancer. *N. Engl. J. Med.* 373:123–135. https://doi.org/10.1056/NEJMoa1504627

Campbell, J.J., G. Haraldsen, J. Pan, J. Rottman, S. Qin, P. Ponath, D.P. Andrew, R. Warnke, N. Ruffing, N. Kassam, et al. 1999. The chemokine receptor CCR4 in vascular recognition by cutaneous but not intestinal memory T cells. *Nature.* 400:776–780. https://doi.org/10.1038/23495

Campbell, J.J., D.J. O'Connell, and M.A. Wurbel. 2007. Cutting Edge: Chemokine receptor CCR4 is necessary for antigen-driven cutaneous accumulation of CD4 T cells under physiological conditions. *J. Immunol.* 178:3358–3362. https://doi.org/10.4049/jimmunol.178.6.3358

Castellino, F., A.Y. Huang, G. Altan-Bonnet, S. Stoll, C. Scheinecker, and R.N. Germain. 2006. Chemokines enhance immunity by guiding naive CD8+ T cells to sites of CD4+ T cell-dendritic cell interaction. *Nature.* 440:890–895. https://doi.org/10.1038/nature04651

Cooper, H.S., S.N. Murthy, R.S. Shah, and D.J. Sedergran. 1993. Clinicopathologic study of dextran sulfate sodium experimental murine colitis. *Lab. Invest.* 69:238–249.

Curiel, T.J. 2008. Regulatory T cells and treatment of cancer. *Curr. Opin. Immunol.* 20:241–246. https://doi.org/10.1016/j.coi.2008.04.008

Curiel, T.J., G. Coukos, L. Zou, X. Alvarez, P. Cheng, P. Mottram, M. Evdemon-Hogan, J.R. Conejo-Garcia, L. Zhang, M. Burow, et al. 2004. Specific recruitment of regulatory T cells in ovarian carcinoma fosters immune privilege and predicts reduced survival. *Nat. Med.* 10:942–949. https://doi.org/10.1038/nm1093

D'Ambrosio, D., C. Albanesi, R. Lang, G. Girolomoni, F. Sinigaglia, and C. Laudanna. 2002. Quantitative differences in chemokine receptor engagement generate diversity in integrin-dependent lymphocyte adhesion. *J. Immunol.* 169:2303–2312. https://doi.org/10.4049/jimmunol.169.5.2303

Förster, R., A. Schubel, D. Breitfeld, E. Kremmer, I. Renner-Müller, E. Wolf, and M. Lipp. 1999. CCR7 coordinates the primary immune response by establishing functional microenvironments in secondary lymphoid organs. *Cell.* 99:23–33. https://doi.org/10.1016/S0092-8674(00)80059-8

Gunn, M.D., S. Kyuwa, C. Tam, T. Kakiuchi, A. Matsuzawa, L.T. Williams, and H. Nakano. 1999. Mice lacking expression of secondary lymphoid organ chemokine have defects in lymphocyte homing and dendritic cell localization. *J. Exp. Med.* 189:451–460. https://doi.org/10.1084/jem.189.3.451

Halin, C., M.L. Scimone, R. Bonasio, J.M. Gauguet, T.R. Mempel, E. Quackenbush, R.L. Proia, S. Mandala, and U.H. von Andrian. 2005. The S1P-analog FTY720 differentially modulates T-cell homing via HEV: T-cell-expressed S1P1 amplifies integrin activation in peripheral lymph nodes but not in Peyer patches. *Blood.* 106:1314–1322. https://doi.org/10.1182/blood-2004-09-3687

Hao, S., X. Han, D. Wang, Y. Yang, Q. Li, X. Li, and C.H. Qiu. 2016. Critical role of CCL22/CCR4 axis in the maintenance of immune homeostasis during apoptotic cell clearance by splenic CD8α(+) CD103(+) dendritic cells. *Immunology.* 148:174–186. https://doi.org/10.1111/imm.12596

Heiseke, A.F., A.C. Faul, H.A. Lehr, I. Förster, R.M. Schmid, A.B. Krug, and W. Reindl. 2012. CCL17 promotes intestinal inflammation in mice and counteracts regulatory T cell-mediated protection from colitis. *Gastroenterology.* 142:335–345. https://doi.org/10.1053/j.gastro.2011.10.027

Iellem, A., L. Colantonio, S. Bhakta, S. Sozzani, A. Mantovani, F. Sinigaglia, and D. D'Ambrosio. 2000. Inhibition by IL-12 and IFN-alpha of I-309 and macrophage-derived chemokine production upon TCR triggering of human Th1 cells. *Eur. J. Immunol.* 30:1030–1039. https://doi.org/10.1002/(SICI)1521-4141(200004)30:4<1030::AID-IMMU1030>3.0.CO;2-8

Iellem, A., M. Mariani, R. Lang, H. Recalde, P. Panina-Bordignon, F. Sinigaglia, and D. D'Ambrosio. 2001. Unique chemotactic response profile and specific expression of chemokine receptors CCR4 and CCR8 by CD4(+) CD25(+) regulatory T cells. *J. Exp. Med.* 194:847–853. https://doi.org/10.1084/jem.194.6.847

Imai, T., D. Chantry, C.J. Raport, C.L. Wood, M. Nishimura, R. Godiska, O. Yoshie, and P.W. Gray. 1998. Macrophage-derived chemokine is a functional ligand for the CC chemokine receptor 4. *J. Biol. Chem.* 273:1764–1768. https://doi.org/10.1074/jbc.273.3.1764

Ishida, T., and R. Ueda. 2006. CCR4 as a novel molecular target for immunotherapy of cancer. *Cancer Sci.* 97:1139–1146. https://doi.org/10.1111/j.1349-7006.2006.00307.x

Lahl, K., C. Loddenkemper, C. Drouin, J. Freyer, J. Arnason, G. Eberl, A. Hamann, H. Wagner, J. Huehn, and T. Sparwasser. 2007. Selective depletion of Foxp3+ regulatory T cells induces a scurfy-like disease. *J. Exp. Med.* 204:57–63. https://doi.org/10.1084/jem.20061852

Larkin, J., V. Chiarion-Sileni, R. Gonzalez, J.J. Grob, C.L. Cowey, C.D. Lao, D. Schadendorf, R. Dummer, M. Smylie, P. Rutkowski, et al. 2015. Combined Nivolumab and Ipilimumab or Monotherapy in Untreated Melanoma. *N. Engl. J. Med.* 373:23–34. https://doi.org/10.1056/NEJMoa1504030

Lee, I., L. Wang, A.D. Wells, M.E. Dorf, E. Ozkaynak, and W.W. Hancock. 2005. Recruitment of Foxp3+ T regulatory cells mediating allograft tolerance depends on the CCR4 chemokine receptor. *J. Exp. Med.* 201:1037–1044. https://doi.org/10.1084/jem.20041709

Levine, A.G., A. Arvey, W. Jin, and A.Y. Rudensky. 2014. Continuous requirement for the TCR in regulatory T cell function. *Nat. Immunol.* 15:1070–1078. https://doi.org/10.1038/ni.3004

Mantovani, A., P.A. Gray, J. Van Damme, and S. Sozzani. 2000. Macrophage-derived chemokine (MDC). *J. Leukoc. Biol.* 68:400–404.

Mempel, T.R., S.E. Henrickson, and U.H. Von Andrian. 2004. T-cell priming by dendritic cells in lymph nodes occurs in three distinct phases. *Nature.* 427:154–159. https://doi.org/10.1038/nature02238

Merad, M., P. Sathe, J. Helft, J. Miller, and A. Mortha. 2013. The dendritic cell lineage: ontogeny and function of dendritic cells and their subsets in the steady state and the inflamed setting. *Annu. Rev. Immunol.* 31:563–604. https://doi.org/10.1146/annurev-immunol-020711-074950

Misra, N., J. Bayry, S. Lacroix-Desmazes, M.D. Kazatchkine, and S.V. Kaveri. 2004. Cutting edge: human CD4+CD25+ T cells restrain the maturation and antigen-presenting function of dendritic cells. *J. Immunol.* 172: 4676–4680. https://doi.org/10.4049/jimmunol.172.8.4676

Montane, J., L. Bischoff, G. Soukhatcheva, D.L. Dai, G. Hardenberg, M.K. Levings, P.C. Orban, T.J. Kieffer, R. Tan, and C.B. Verchere. 2011. Prevention of murine autoimmune diabetes by CCL22-mediated Treg recruitment to the pancreatic islets. *J. Clin. Invest.* 121:3024–3028. https://doi.org/10.1172/JCI43048

Onishi, Y., Z. Fehervari, T. Yamaguchi, and S. Sakaguchi. 2008. Foxp3+ natural regulatory T cells preferentially form aggregates on dendritic cells in vitro and actively inhibit their maturation. *Proc. Natl. Acad. Sci. USA.* 105:10113–10118. https://doi.org/10.1073/pnas.0711106105

Pardoll, D.M. 2012. The blockade of immune checkpoints in cancer immunotherapy. *Nat. Rev. Cancer.* 12:252–264. https://doi.org/10.1038/nrc3239

Pere, H., Y. Montier, J. Bayry, F. Quintin-Colonna, N. Merillon, E. Dransart, C. Badoual, A. Gey, P. Ravel, E. Marcheteau, et al. 2011. A CCR4 antagonist combined with vaccines induces antigen-specific CD8+ T cells and tumor immunity against self antigens. *Blood.* 118:4853–4862. https://doi.org/10.1182/blood-2011-01-329656

Rapp, M., S. Grassmann, M. Chaloupka, P. Layritz, S. Kruger, S. Ormanns, F. Rataj, K.P. Janssen, S. Endres, D. Anz, and S. Kobold. 2015. C-C chemokine receptor type-4 transduction of T cells enhances interaction with dendritic cells, tumor infiltration and therapeutic efficacy of adoptive T cell transfer. *OncoImmunology.* 5:e1105428. https://doi.org/10.1080/2162402X.2015.1105428

Romagnani, S. 2002. Cytokines and chemoattractants in allergic inflammation. *Mol. Immunol.* 38:881–885. https://doi.org/10.1016/S0161-5890(02)00013-5

Rot, A., and U.H. von Andrian. 2004. Chemokines in innate and adaptive host defense: basic chemokinese grammar for immune cells. *Annu. Rev. Immunol.* 22:891–928. https://doi.org/10.1146/annurev.immunol.22.012703.104543

Sakaguchi, S., K. Wing, Y. Onishi, P. Prieto-Martin, and T. Yamaguchi. 2009. Regulatory T cells: how do they suppress immune responses? *Int. Immunol.* 21:1105–1111. https://doi.org/10.1093/intimm/dxp095

Sather, B.D., P. Treuting, N. Perdue, M. Miazgowicz, J.D. Fontenot, A.Y. Rudensky, and D.J. Campbell. 2007. Altering the distribution of Foxp3(+) regulatory T cells results in tissue-specific inflammatory disease. *J. Exp. Med.* 204:1335–1347. https://doi.org/10.1084/jem.20070081

Schajnovitz, A., T. Itkin, G. D'Uva, A. Kalinkovich, K. Golan, A. Ludin, D. Cohen, Z. Shulman, A. Avigdor, A. Nagler, et al. 2011. CXCL12 secretion by bone marrow stromal cells is dependent on cell contact and mediated by connexin-43 and connexin-45 gap junctions. *Nat. Immunol.* 12: 391–398. https://doi.org/10.1038/ni.2017

Schaniel, C., E. Pardali, F. Sallusto, M. Speletas, C. Ruedl, T. Shimizu, T. Seidl, J. Andersson, F. Melchers, A.G. Rolink, and P. Sideras. 1998. Activated murine B lymphocytes and dendritic cells produce a novel CC chemokine which acts selectively on activated T cells. *J. Exp. Med.* 188:451–463. https://doi.org/10.1084/jem.188.3.451

Schneider, M.A., J.G. Meingassner, M. Lipp, H.D. Moore, and A. Rot. 2007. CCR7 is required for the in vivo function of CD4+ CD25+ regulatory T cells. *J. Exp. Med.* 204:735–745. https://doi.org/10.1084/jem.20061405

Scimone, M.L., T.W. Felbinger, I.B. Mazo, J.V. Stein, U.H. Von Andrian, and W. Weninger. 2004. CXCL12 mediates CCR7-independent homing of central memory cells, but not naive T cells, in peripheral lymph nodes. *J. Exp. Med.* 199:1113–1120. https://doi.org/10.1084/jem.20031645

Shen, Z., G. Reznikoff, G. Dranoff, and K.L. Rock. 1997. Cloned dendritic cells can present exogenous antigens on both MHC class I and class II molecules. *J. Immunol.* 158:2723–2730.

Smigiel, K.S., S. Srivastava, J.M. Stolley, and D.J. Campbell. 2014. Regulatory T-cell homeostasis: steady-state maintenance and modulation during inflammation. *Immunol. Rev.* 259:40–59. https://doi.org/10.1111/imr.12170

Sugiyama, D., H. Nishikawa, Y. Maeda, M. Nishioka, A. Tanemura, I. Katayama, S. Ezoe, Y. Kanakura, E. Sato, Y. Fukumori, et al. 2013. Anti-CCR4 mAb selectively depletes effector-type FoxP3+CD4+ regulatory T cells, evoking antitumor immune responses in humans. *Proc. Natl. Acad. Sci. USA.* 110:17945–17950. https://doi.org/10.1073/pnas.1316796110

Tadokoro, C.E., G. Shakhar, S. Shen, Y. Ding, A.C. Lino, A. Maraver, J.J. Lafaille, and M.L. Dustin. 2006. Regulatory T cells inhibit stable contacts between CD4+ T cells and dendritic cells in vivo. *J. Exp. Med.* 203: 505–511. https://doi.org/10.1084/jem.20050783

Tang, H.L., and J.G. Cyster. 1999. Chemokine Up-regulation and activated T cell attraction by maturing dendritic cells. *Science.* 284:819–822. https://doi.org/10.1126/science.284.5415.819

Tang, Q., J.Y. Adams, A.J. Tooley, M. Bi, B.T. Fife, P. Serra, P. Santamaria, R.M. Locksley, M.F. Krummel, and J.A. Bluestone. 2006. Visualizing regulatory T cell control of autoimmune responses in nonobese diabetic mice. *Nat. Immunol.* 7:83–92. https://doi.org/10.1038/ni1289

Vitali, C., F. Mingozzi, A. Broggi, S. Barresi, F. Zolezzi, J. Bayry, G. Raimondi, I. Zanoni, and F. Granucci. 2012. Migratory, and not lymphoid-resident, dendritic cells maintain peripheral self-tolerance and prevent autoimmunity via induction of iTreg cells. *Blood.* 120:1237–1245. https://doi.org/10.1182/blood-2011-09-379776

Vulcano, M., C. Albanesi, A. Stoppacciaro, R. Bagnati, G. D'Amico, S. Struyf, P. Transidico, R. Bonecchi, A. Del Prete, P. Allavena, et al. 2001. Dendritic cells as a major source of macrophage-derived chemokine/CCL22 in vitro and in vivo. *Eur. J. Immunol.* 31:812–822. https://doi.org/10.1002/1521-4141(200103)31:3<812::AID-IMMU812>3.0.CO;2-L

Wing, K., Y. Onishi, P. Prieto-Martin, T. Yamaguchi, M. Miyara, Z. Fehervari, T. Nomura, and S. Sakaguchi. 2008. CTLA-4 control over Foxp3+ regulatory T cell function. *Science.* 322:271–275. https://doi.org/10.1126/science.1160062

Wu, M., H. Fang, and S.T. Hwang. 2001. Cutting edge: CCR4 mediates antigen-primed T cell binding to activated dendritic cells. *J. Immunol.* 167:4791–4795. https://doi.org/10.4049/jimmunol.167.9.4791

Yuan, Q., S.K. Bromley, T.K. Means, K.J. Jones, F. Hayashi, A.K. Bhan, and A.D. Luster. 2007. CCR4-dependent regulatory T cell function in inflammatory bowel disease. *J. Exp. Med.* 204:1327–1334. https://doi.org/10.1084/jem.20062076

Zhou, G., C.G. Drake, and H.I. Levitsky. 2006. Amplification of tumor-specific regulatory T cells following therapeutic cancer vaccines. *Blood.* 107: 628–636. https://doi.org/10.1182/blood-2005-07-2737

Zou, W. 2006. Regulatory T cells, tumour immunity and immunotherapy. *Nat. Rev. Immunol.* 6:295–307. https://doi.org/10.1038/nri1806